JOURNAL OF CATALYSIS 84, 308–316 (1983)

Role of Carriers in the Production of Hydrogen from Water by Reduction–Oxidation Cycle of In_2O_3

KIYOSHI OTSUKA, SHIN-ICHI SHIBUYA, AND AKIRA MORIKAWA

Department of Chemical Engineering, Tokyo Institute of Technology, Ookayama, Meguro-ku, Tokyo 152, Japan

Received January 5, 1983; revised May 25, 1983

The promoting effects of various carriers on the decomposition of water by reduction–oxidation cycle of In_2O_3 have been examined. The most favorable carriers were ZrO_2, TiO_2, and MgO. Reduction and oxidation of indium oxide can be explained by "homogeneous model" which assumes rapid diffusion of oxygen ions from the surface of indium oxide grains into the bulk or vice versa, resulting in a homogeneous distribution of oxygen ions and indium metal. The promoting effect of carriers on reduction of In_2O_3 can be ascribed to the dispersion and stabilization of In_2O_3 grains on their surfaces. The effect of carriers on oxidation of the reduced indium oxide accompanying decomposition of water was explained by the activation of water molecules adsorbed at the boundary of indium oxide and carriers. The water molecules may be strongly polarized by the strong electrostatic field generated at the boundary.

INTRODUCTION

Recently we have described a simple two-step water decomposition process which uses a reduction (step 1) and oxidation (step 2) cycle of In_2O_3 (*1–4*):

Step 1: In_2O_3 + reductant → 2In + oxidized product

Step 2: $2In + 3H_2O \rightarrow In_2O_3 + 3H_2$

The reductant in step 1 could be hydrogen, carbon monoxide, carbon, methane, or biomass (*1–4*). In step 2, the metallic indium produced in step 1 is reoxidized by water thus producing hydrogen (*2, 4*). The reduction of In_2O_3 powder by hydrogen or carbon monoxide and the subsequent decomposition of water proceed smoothly at 673 K (*2*). However, higher reactivity of the oxide is desired in order to operate the cycle at lower temperatures. Moreover, the reactivity is required to be maintained for repeated cycles.

Carriers have many distinct functions in improving the quality of reactive solids. They enable a better dispersion of the supported active agent and prevent its sintering during the redox cycles. They sometimes possess their own catalytic activities, which increase the overall efficiency of the catalyst. They also modify many properties of the deposited compounds. The effect may be either favorable or deleterious. In this work, we first describe the experimental survey of carriers of In_2O_3 effective to enhance the rates of reduction and reoxidation of indium oxide. Second, the mechanism of reduction and reoxidation will be proposed on the basis of kinetic studies of the reactions. Finally, the role of carriers will be discussed.

EXPERIMENTAL

Materials. The In_2O_3 without carriers was prepared by the decomposition of $In(NO_3)_3$ in a flow of nitrogen gas at 773 K. The In_2O_3 supported on various carriers were prepared by the decomposition of $In(NO_3)_3$ on the carriers in a vacuum at 773 K. The $In(NO_3)_3$ was impregnated into the carriers from its aqueous solution. The weight percentage of the supported In_2O_3 was usually adjusted to 11.1%. The

0021-9517/83 $3.00

$In(NO_3)_3$ and the various carriers used were obtained from Wako Pure Chemical Company, Soekawa Chemical Company, Koso Chemical Company, Davison Chemical Company, or Merk. The hydrogen and carbon monoxide used as reducing gases were purified by passing them through a silica-gel cooled at 77 or 195 K. The water was purified three times by trap-to-trap distillation in a vacuum apparatus. Dissolved gases in the water were removed by repeated freeze-degassing-thaw procedure.

Procedure. The apparatus employed was a conventional mercury-free, grease-free, static gas-circulation system with 285 cm^3 volume. The surface areas of carriers were measured by means of BET method applying nitrogen adsorption at 77 K. Before each experiment of step 1, the In_2O_3 with or without carrier (50–500 mg) in a U-shaped quarts reactor was calcined in an atmosphere of oxygen (1.3×10^4 Pa) at 773 K and degassed for 2 h at the same temperature. The reduction of the sample was initiated by adding hydrogen or carbon monoxide to the system at 473–673 K. The water or carbon dioxide in the gas phase produced during the reduction were always removed by condensing them into a trap which had been placed in the gas-circulation line and cooled at 77 K by liquid nitrogen. Kinetic curves of the reduction under various reaction conditions were obtained from the pressure drop of the reducing gas. The initial pressure of the reducing gas was usually 13.0 ± 0.2 kPa and the final pressure of the reducing gas was not lower than 12 kPa. The reoxidation of the reduced indium oxide by water (step 2) was carried out by adding and circulating a mixture of water vapor (2.1 kPa) and nitrogen (6.7 kPa, added to ensure gas circulation) at 473–673 K. The quantity of produced hydrogen was measured by gas chromatography using active carbon as a solid support. The kinetic studies of the reoxidation for the indium oxide supported on TiO_2 were carried out with the sample preliminarily reduced to 58 ± 1% degree of reduction.

RESULTS

Comparison of the Rates of Step 1 Among the Different Samples

Before the experiments for the supported In_2O_3 samples, the reduction of carriers by hydrogen was examined at the temperatures of 673–873 K. As one imagines, no reduction was observed for the Al_2O_3, SiO_2, $SiO_2 \cdot Al_2O_3$, MgO, ZrO_2, and La_2O_3. Reduction of the TiO_2 (anatase, from Merk) or of the ZnO (from Koso Chemical Co.) did not occur at all at <873 K. Reduction of the WO_3 (from Wako Pure Chemical Co.) commenced at >723 K.

The rates of reduction by hydrogen have been measured for the supported In_2O_3 under the hydrogen pressure of 13–12 kPa. Since the experiments were carried out at 423–673 K, the participation of carriers to the reduction could be neglected. The kinetic curves of consumption of hydrogen observed for the In_2O_3 samples supported on Al_2O_3, SiO_2, $SiO_2 \cdot Al_2O_3$, MgO, and La_2O_3 indicated that very fast consumption of hydrogen occurred at the very initial stage of the reaction. This rather unusual consumption of hydrogen was followed by a slow but steady one. The first-order plots of the steady reaction at 623 K are shown in Fig. 1 for the samples of different carriers. The α in $\log(1 - \alpha)$ of the vertical axis is the degree of reduction of In_2O_3 evaluated from the ratio of the quantity of oxygen atoms removed from the oxide in time t to that contained in fresh In_2O_3. Usually the former was estimated as the quantity of consumed hydrogen gas. The samples displayed unusually rapid, initial consumption of hydrogen, the quantity used for the reduction of oxide was evaluated by subtracting the amount of the unusual hydrogen from that of hydrogen gas consumed in time t. The former was estimated by extrapolation of the smooth kinetic curves of steady reaction to time zero. The hydrogen consumed very rapidly at the initial stage of the reaction was assumed not effective to the reduction of In_2O_3. This assumption was

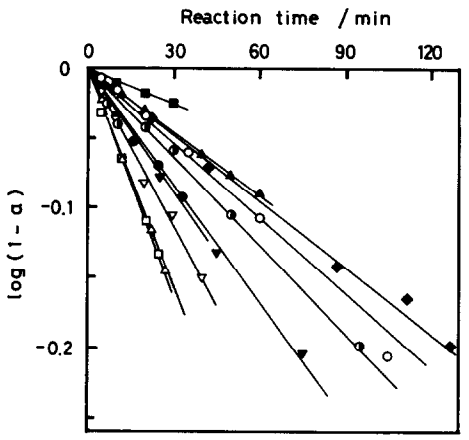

FIG. 1. First-order plots of reduction of In_2O_3 on different carriers by hydrogen at 673 K: ○, In_2O_3 alone; ◆, Pt-black mixed. Carriers: ■, Al_2O_3; ▲, $SiO_2 \cdot Al_2O_3$; ◑, WO_3; ×, SiO_2; ▼, graphite; ▽, La_2O_3; □, TiO_2; △, ZrO_2.

supported by the observation that the In_2O_3/Al_2O_3 and In_2O_3/MgO, after an initial rapid consumption of hydrogen without a subsequent steady reduction, did not decompose water in step 2. This hydrogen might be the one adsorbed or spilled over to the carriers.

As can be seen in Fig. 1 the first-order plot gave good straight lines for all of the samples examined at 623 K. However, for the samples such as In_2O_3/WO_3, In_2O_3/SiO_2, In_2O_3/Al_2O_3, or $In_2O_3/SiO_2 \cdot Al_2O_3$ at the reaction temperatures less than 573 K, the plot indicated concave curves. The rates of reduction, which were evaluated from the slopes of the first-order plot multiplied by the amount of oxygen atoms in In_2O_3 (1.08×10^{-2} mol-atom g^{-1}), have been shown in Table 1. For the samples listed below the row of In_2O_3/La_2O_3 in Table 1, no or very small enhancing effect of carriers on the rates was observed compared to that of In_2O_3 without carrier. However, considerable promotion has been found for the carriers ZnO, MgO, active carbon, ZrO_2, and TiO_2.

TABLE 1

Surface Areas of Carriers, Weight Percentage of In_2O_3 Supported, and the Rates of Step 1

In_2O_3/carrier	Surface area of carrier ($m^2\ g^{-1}$)	Weight % of In_2O_3 supported on carriers	Rate of reduction (10^{-7} mol $H_2\ s^{-1}$)	
			573 K	623 K
In_2O_3 alone	9		3.38	7.48
In_2O_3/ZnO	6	11.1	19.7	[c]
In_2O_3/MgO	251	11.1	13.0	[c]
In_2O_3/active carbon	941	28.1	9.55	[c]
In_2O_3/ZrO_2	29	11.1	8.85	21.6
In_2O_3/TiO_2	11	11.1	8.16	22.7
In_2O_3/La_2O_3	[c]	11.1	4.70	15.8
In_2O_3/graphite	[c]	11.1	5.46	11.7
$In_2O_3/SiO_2 \cdot Al_2O_3$	511	13.0	[b]	6.36
In_2O_3/SiO_2	655	19.2	[b]	11.9
Pt-black mixed	[c]	6.1[a]	3.46	6.57
In_2O_3/WO_3	7	11.1	[b]	8.78
In_2O_3/Al_2O_3	237	11.1	[b]	3.60

[a] Weight percentage of Pt-black mixed with In_2O_3.
[b] The rate could not be evaluated because the data did not fit the first-order plot.
[c] Not measured.

TABLE 2

Initial Degrees of Reduction, the Final H_2 yield, and the Rates of H_2 production in Step 2

In_2O_3/carrier	Initial degree of reduction (%)	Final H_2 yield (%)	Rate of H_2 production (10^{-7} mol H_2 s^{-1}) (at 473 K)
In_2O_3 alone	57.6	103	0.43
In_2O_3/ZrO_2	57.3	98	8.04
In_2O_3/TiO_2	58.2	100	7.68
In_2O_3/Al_2O_3	27.7	87	7.04
In_2O_3/MgO	47.9	104	5.00
In_2O_3/active carbon	32.7	90	4.27[a]
In_2O_3/ZnO	58.2	93	2.57
In_2O_3/La_2O_3	47.7	51	2.17
In_2O_3/SiO_2	23.6	42	1.03[a]
Pt-black mixed	52.8	82	0.77
In_2O_3/graphite	60.3	74	0.74
$In_2O_3/SiO_2 \cdot Al_2O_3$	26.6	33	0.56
In_2O_3/WO_3	55.0	13	0.02

[a] Evaluated from the dotted line in Fig. 2.

Comparison of the Rates of Hydrogen Formation (Step 2)

The rates of reoxidation of the reduced indium oxides by water have been measured at 473–673 K. Before the reoxidation, the samples had been reduced by hydrogen at 623 K until the degrees of reduction of the oxides shown on the second column in Table 2 were obtained. For every sample tested, the formation of hydrogen at 673 K was rapid and completed within 60 min. The percentages of the recovered hydrogen compared to that used for reduction in step 1 (the quantity of the rapid consumption of hydrogen at the very initial stages of step 1 was excluded) are shown in the third column of Table 2.

The kinetic curves of hydrogen production have been fitted to first-order plot. The data obtained at 473 K are plotted in Fig. 2, where β is the ratio of the amount of hydrogen produced at time t to that of the hydrogen finally recovered as described above. As can be seen in Fig. 2, good straight lines are observed for most of the samples, but for In_2O_3/SiO_2 and In_2O_3/active carbon the plot gave concave curves. However, when temperature was raised to 573 K, good straight lines were observed for these two samples. The rates of hydrogen production, which were evaluated from the slopes of the straight lines multiplied by the final yields of hydrogen, are indicated in the last column of Table 2. The results in the last column show that most of the carriers have favorable effects on the rates of hydrogen production. The final yields of hydrogen for pure In_2O_3, In_2O_3/ZrO_2, In_2O_3/TiO_2, and In_2O_3/MgO in the third column of Table 2 indicate that the hydrogen consumed on step 1 is almost recovered on step 2 within experimental error (±3% yield). The recoveries for In_2O_3/ZnO, In_2O_3/active carbon, and In_2O_3/Al_2O_3 are also good.

Kinetic Studies with In_2O_3/TiO_2

As described above, TiO_2 carrier showed high final yield of hydrogen and high enhancing effects on both rates of reduction and oxidation of In_2O_3. Hence, the kinetic studies of the reactions have been performed on the In_2O_3/TiO_2 sample chosen as a typical example of supported In_2O_3.

(a) Effect of pressure of hydrogen or water vapor on the rate of reaction. Effect of

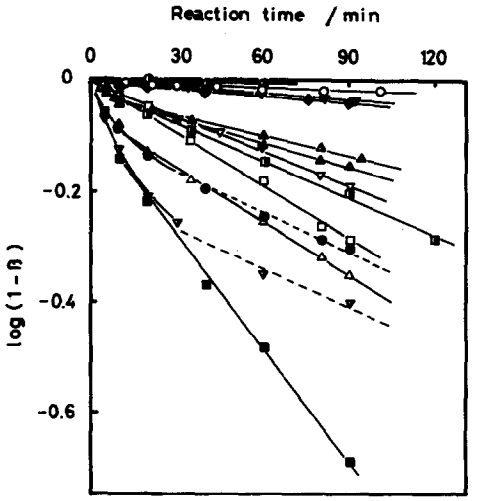

FIG. 2. First-order plots of reoxidation of the reduced indium oxide on different carriers at 473 K: ○, In_2O_3 alone; ◆, Pt-black mixed. Carriers: ◑, WO_3; ▼, graphites; Δ, ZnO; ▲, $SiO_2 \cdot Al_2O_3$: ▽, La_2O_3; ◨, MgO; □, TiO_2; ●, SiO_2; △, ZrO_2; ▽, active carbon; ■, Al_2O_3.

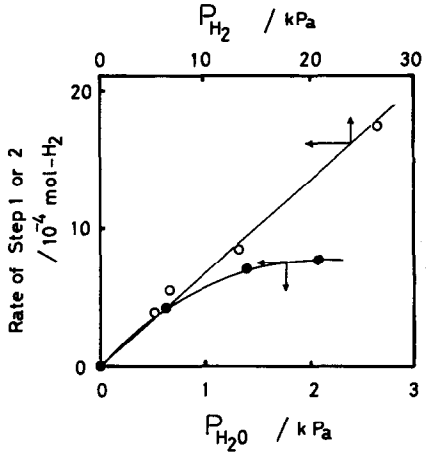

FIG. 3. Effect of pressure of reactant in the gas phase on the rates of steps 1 and 2: step 1 at 573 K and step 2 at 473 K. ○, Step 1; ●, step 2.

pressure of reactant gas on the rate of reduction or reoxidation of the sample is indicated in Fig. 3. The reduction and oxidation were carried out at 573 and 473 K, respectively. The rate of reduction was proportional to the pressure of hydrogen, but the rate of oxidation reached a plateau at about 2.0 kPa.

(*b*) *Reducing power of CO.* The kinetic feature of reduction of In_2O_3/TiO_2 by carbon monoxide was very similar to that by hydrogen. The kinetic curve of reduction by carbon monoxide also well fitted to the first-order plot. The rate of reduction by carbon monoxide, however, was 1.6 times faster than that by hydrogen at 573 K. There was no difference in the rates of reoxidation by water vapor between the samples reduced by carbon monoxide and by hydrogen.

(*c*) *Effect of the number of reduction–oxidation cycles.* The changes in the kinetic curves of reduction and oxidation by repetition of reaction cycles have been examined for pure In_2O_3 (Figs. 4a and a′) and In_2O_3/TiO_2 (Figs. 4b and b′). Before each reduction experiment with hydrogen, the samples tested in step 2 had been calcined under 13.3 kPa of pure oxygen at 773 K. After the step 1 experiment at 573 K as shown in Figs. 4a and b, the sample was further reduced to the 56–58% level at 623 K before each step 2 experiment. Reduction of In_2O_3 without carrier became very slow at 573 K on second and third cycles, though it occurred appreciably on the first reduction (Fig. 4a). However, when the temperature was raised to 623 K, reductions on second and third cycles proceeded smoothly though the rates decreased to 64 and 49% of that of the first one, respectively. Reduction of In_2O_3 on TiO_2 proceeded smoothly on second and third cycles at 573 K, though the rates of reaction decreased to half of that observed at the first cycle (Fig. 4b). In the case of step 2, the reactivity of reduced indium oxide without carrier decreased considerably after each reduction cycle (Fig. 4a′). However, the drop in activity was lessened when the oxide was supported on TiO_2 as can be seen in Fig. 4b′.

DISCUSSION

Topochemical Reaction Models

Reduction of an oxide with a reducing gas such as hydrogen or carbon monoxide is an example of a topochemical reaction of

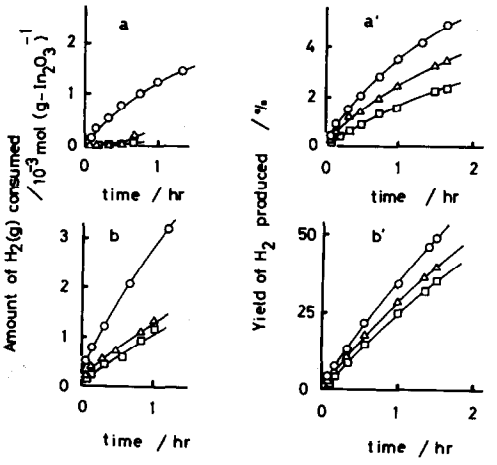

FIG. 4. Effect of repeated reduction–oxidation cycles: step 1 at 573 K and step 2 at 473 K. (a) In_2O_3 alone (step 1); (a′) reduced In_2O_3 (step 2); (b) In_2O_3/TiO_2 (step 1); (b′) reduced In_2O_3/TiO_2 (step 2). Number of cycle: ○, first; △, second; □, third cycle.

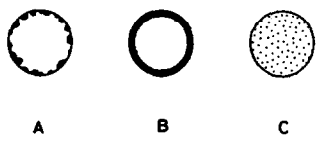

FIG. 5. Schematic topochemical reaction models: (A) formation and growth of nuclei model; (B) shrinking sphere model; (C) homogeneous model.

the type: solid(1) + gas(1) = solid(2) + gas(2). The characteristic feature of a topochemical reaction is the fact that it is localized at the interface between solid substrate and solid product, which is called the reaction interface, in contrast to a homogeneous reaction, which proceeds in the whole volume.

It is convenient to discuss a topochemical reaction by dividing it into two parts. One is the discussion of how the reaction interface changes in the course of the reaction. The other is the discussion of the rate of chemical reaction per unit surface area of the reaction interface. The rate measured experimentally may thus be expressed as follows:

$$R = r(c_i, T) \cdot S(t) \qquad (1)$$

where r is the rate of chemical reaction and S is the surface area of the reaction interface.

Let us first consider the changes of the reaction interface in the course of the reaction. When the solid is contacted with the reactant in the gas phase, the reaction starts, and after a certain time the interface grows in the form of crystal nuclei of the solid product. The nuclei enhance the reactivity in their vicinity as a result of various interface effects (e.g., appearance of more reactive faces, catalytic action of solid products). The reaction interface begins now to increase more and more rapidly due to two processes, i.e., growth of the nuclei already formed and appearance of new ones. The phenomena will correspond to what is usually called a process of "formation and growth of nuclei" (schematic model A in Fig. 5). For this reaction model a typical sigmoidal curve of the dependence of the conversion on time can be obtained (5).

In many cases, however, nucleation is very rapid and a thin layer of the product covers the substrate grains in the very early stage of the reaction. The reaction interface decreases continuously from the beginning of reaction with the progress of reaction into the substrate grains. This model is often called the "shrinking sphere model" (model B in Fig. 5). For this reaction model the dependence of conversion α on time is given by a formula:

$$(1 - \alpha)^{1/3} = -kt + 1 \qquad (2)$$

where k is the rate constant of the reaction.

If there is no change in the reaction interface and the product diffuses rapidly from the reaction interface at surface into the bulk of substrate grains, resulting in a homogeneous distribution of the product both at the surface and in the bulk of the grains during reaction ("homogeneous model" C in Fig. 5), the relation between α and time can be expressed as follows:

$$\ln(1 - \alpha) = -kt + C \qquad (3)$$

where C is a constant.

The observed kinetic curves fitted to neither a sigmoidal curve nor the Eq. (2). Most of the experimental curves fitted well to Eq. (3) in both cases of reduction and oxidation as described earlier. This suggests that the homogeneous sphere model is the most probable reaction model for the $H_2O/In/In_2O_3/H_2$ system.

The rate constant k in Eq. (3) depends on the inverse of diameter of In_2O_3 grains. Therefore, nonuniformity of the grain size of In_2O_3 may have caused the deviation of experimental points from the linear correlation of $\log(1 - \alpha)$ vs time plot, which was observed for the In_2O_3/active carbon and In_2O_3/SiO_2 in Fig. 2 and for the samples tested in step 1 at <573 K such as In_2O_3/WO_3, In_2O_3/SiO_2, In_2O_3/Al_2O_3, or $In_2O_3/SiO_2 \cdot Al_2O_3$. The growth of grain size of In_2O_3 by repeated reduction–oxidation cy-

cles should decrease the reaction rate as demonstrated in Fig. 4.

Let us now discuss the second question concerning the chemical reaction occuring at unit surface area of indium oxide. Although detailed kinetic studies have not been made at the moment, the reduction and oxidation may tentatively be described as the forward and the reverse of the following equations, respectively:

$$H_2(g) \rightleftarrows 2H(ads) \quad (4)$$

$$2H(ads) + \tfrac{1}{3}In_2O_3(surface) \rightleftarrows H_2O(ads) + \tfrac{2}{3}In(surface) \quad (5)$$

$$H_2O(ads) \rightleftarrows H_2O(g) \quad (6)$$

$$\tfrac{2}{3}In(surface) + V_{\ddot{O}}(surface) + O^{2-}(surface) \rightleftarrows \tfrac{1}{3}In_2O_3(surface) \quad (7)$$

$$O^{2-}(bulk) \rightleftarrows O^{2-}(surface) \quad (8)$$

$$V_{\ddot{O}}(bulk) \rightleftarrows V_{\ddot{O}}(surface) \quad (9)$$

$$\tfrac{1}{3}In_2O_3(bulk) \rightleftarrows \tfrac{2}{3}In(bulk) + V_{\ddot{O}}(bulk) + O^{2-}(bulk) \quad (10)$$

where Eq. (8) means the rapid diffusion of oxygen ions accompanied by that of the oxygen ion vacancies, $V_{\ddot{O}}$ (Eq. (9)) from the bulk to the surface, or vice versa, ensuring homogeneous distribution of the In metal. We cannot exclude the possibility that hydrogen in the gas phase attacks In_2O_3 directly in Eq. (5) since the rate of reduction depends proportionally on the pressure of hydrogen (Fig. 3). In the case of step 2, however, the pressure effect of water vapor as shown in Fig. 3 suggests that the water adsorbed on the reaction interface is a reaction intermediate.

Effect of Carriers on Step 1

One of the favorable effects of carriers on the enhancement of rate of reduction of In_2O_3 may be attributed to their large surface areas on which In_2O_3 grains would be highly dispersed. However, the results in Table 1 indicate that the carriers having high surface areas such as SiO_2, Al_2O_3, or $SiO_2 \cdot Al_2O_3$ enhanced only slightly or rather reduced the rate of reduction. In contrast to those carriers, ZnO, ZrO_2, and TiO_2, though these three have 1 to 2 orders of magnitude lower surface areas, enhanced the activity in reduction considerably.

TABLE 3

Activation Energies of Reduction of In_2O_3 for Different Samples

In_2O_3/carrier	Activation energy (kJ(mol O atom)$^{-1}$)
In_2O_3 alone	68
In_2O_3/TiO_2	66
In_2O_3/ZrO_2	63
In_2O_3/ZnO	74

The activation energies of reduction by hydrogen for some supported samples have been evaluated from the rates of reduction measured in the temperature range 423–673 K. The values are summarized in Table 3. The activation energies are coincident with each other within the experimental error ± 6 kJ. The fact that the carriers do not change the activation energies of the reduction from that of pure In_2O_3 suggests that a chemical modification of indium oxide by carriers is not significant as far as the reduction of In_2O_3 is concerned. The role of effective carriers such as ZnO, MgO, active carbon, ZrO_2, or TiO_2 may be ascribed to a high dispersion and stabilization of small In_2O_3 grains on the surface of the carriers. Strong deactivation in the reduction with repeated cycles of reaction observed for the In_2O_3 without carriers (Fig. 4a) was suppressed considerably when the oxide was supported on TiO_2 (Fig. 4b), suggesting that the carrier would prevent the sintering of In_2O_3 grains during the reaction cycles.

Pt-black is well known as an effective catalyst for dissociating hydrogen. The Pt-black added to In_2O_3, however, did not show any promoting effect on step 1 as can be seen in Table 1. This implies that the activation of hydrogen (e.g., dissociation of $H_2(g)$ or promotion of reactivity of H(ads))

TABLE 4

Electron Affinities (*EA*), Standard Redox Potentials of Carriers (E°), Rates (R), and Activation Energies of Step 2 (E_a) for Different Samples

Sample	*EA*[a] (eV)	E° (vs NHE) (V)	R (10^{-7} (mol H_2) s^{-1}) at 473 K	E_a (kJ (mol H_2)$^{-1}$)
In_2O_3/La_2O_3	—	−1.72	2.17	[b]
In_2O_3/MgO	1.42	−1.70	5.00	[b]
In_2O_3/Al_2O_3	—	−1.47	7.04	41
In_2O_3/ZrO_2	3.42	−1.43	8.04	31
In_2O_3/TiO_2	4.33	−0.86	7.68	48
In_2O_3/SiO_2	—	−0.86	1.03	47
In_2O_3/ZnO	4.15	−0.42	2.57	58
In_2O_3 alone	4.45 (*7*), 5.0 (*8*)	−0.21	0.43	60
In_2O_3/WO_3	5.18	−0.09	0.02	80

[a] From Butler and Ginley (*6*) unless otherwise noted.
[b] Not measured.

is not a rate determining step of reduction.

It is open to question why the carrier of high surface areas such as SiO_2, Al_2O_3, or $SiO_2 \cdot Al_2O_3$ has small or negative promoting effect on the rate of reduction. Further studies are needed to clarify this point.

Effect of Carriers on Step 2

Most of the carriers indicated promoting effect in step 2 as shown in Table 2. Of these, the most effective carriers are ZrO_2, TiO_2, Al_2O_3, and MgO. However, the Al_2O_3 was not effective in step 1. Therefore, for the production of hydrogen by reduction–oxidation cycles, we conclude that the most favorable carriers are ZrO_2, TiO_2, and MgO.

It was generally observed that the effect of carriers was much more pronounced in step 2 than in step 1. Table 4 shows the activation energies of hydrogen production for different supported samples were evaluated from the Arrhenius plot of the rates of reaction observed at 473–673 K. The plot indicated good straight line for every sample. The activation energies are shown on the last column of Table 4. The carriers having high promoting ability on hydrogen production such as ZrO_2, TiO_2, or Al_2O_3 (Table 2) indicated considerably lower activation energies compared to the value of pure In_2O_3 (Table 4). This suggests that a chemical modification of the reaction system is responsible for the promoting effect of the carriers.

When two semiconductors are brought into contact with each other, electrons flow from one semiconductor to the other. The direction of the flow depends on the positions of the Fermi levels of the two semiconductors. The direction can be also predicted by comparison of the electron affinities of the oxides. The electron affinity of a semiconductor will be given by

$$EA = \chi - \tfrac{1}{2}E_g \qquad (11)$$

where χ is the bulk electronegativity of the compound which is the geometric mean of the electronegativities of the constituent atoms, and E_g is the bandgap energy between conduction and valence band levels of the compound (*6*). The values of electron affinities of the carriers are shown in the second column of Table 4.

One of the thermodynamic parameters to predict the ease of oxidation or reduction of a compound is its standard redox potential. Electron transfer from one oxide to the other corresponds to the occurrence of oxidation and reduction of the two compounds. Therefore, if the electron transfer occurs between the two oxides after their

contact, the direction of the transfer may be predicted by their standard redox potentials. Here, the redox reactions are restricted at the surface layers of the oxides, and the electron transfer into the whole oxides should not be considered. Thus, the standard potentials can only be adopted as one of the parameters to suggest the direction of electron transfer between the surface layers of In_2O_3 and carriers. The standard potentials (vs NHE) of the oxides used as carriers are indicated in the third column of Table 4. The potentials are estimated on the basis of oxidation–reduction between the oxides and their elements ($M_xO_y + 2yH^+ + 2ye^- = xM + yH_2O$) (*9*).

The rates of hydrogen production at 473 K are listed again in the fourth column of Table 4 for convenience of comparison. It is noteworthy that the carriers of lower electron affinities or potentials than those of In_2O_3 give lower activation energies compared to that of In_2O_3 without carrier. Consequently, the favorable effects on the rate of hydrogen production are observed for these carriers. In contrast to these carriers, the WO_3 having higher electron negativity and standard potential than those of In_2O_3 gives the large activation energy and, consequently, decreases the reactivity of reduced indium oxide.

The transfer of electrons from the carrier to indium oxide results in buildup of a space charge in a boundary layer extending to a certain depth from the contact interface of indium oxide and carrier. A strong electrostatic field generated around the contact interface would strongly polarize and activate the water molecules adsorbed in the vicinity of the boundary, which explains the promoting effect of the carriers on the decomposition of water. After the activation of water molecules, migration of the activated species (H_2O^*, H^+, or OH^-) to react with indium metal on the surface of reduced indium oxide may strongly depend on the sign (plus or minus) of the space charge at the side of indium oxide. This might be a reason why WO_3 indicated negative effect on water decomposition as described above.

We have no satisfactory explanation of the incomplete recoveries of hydrogen for the samples such as In_2O_3/SiO_2, In_2O_3/La_2O_3, $In_2O_3/SiO_2 \cdot Al_2O_3$, or In_2O_3/WO_3 (Table 2). Since the quantity of the rapid consumption of hydrogen at the very initial stage of reduction in step 1 was excluded in the evaluation of the degree of reduction of In_2O_3, the low final yields of hydrogen for these samples cannot be ascribed to an overestimation of the degree of reduction of In_2O_3. As described earlier, the carriers were never reduced under the reaction conditions applied in this work. We speculate that compound oxides formed between In_2O_3 and carriers are easily reduced, but their reduced states are not able to decompose water.

REFERENCES

1. Otsuka, K., Takizawa, Y., Shibuya, S., and Morikawa, A., *Chem. Lett.* **1981,** 347.
2. Otsuka, K., Yasui, T., and Morikawa, A., *Bull. Chem. Soc. Jpn.* **55,** 1768 (1982).
3. Otsuka, K., Takizawa, Y., and Morikawa, A., *Fuel Process. Technol.* **6,** 215 (1982).
4. Otsuka, K., Yasui, T., and Morikawa, A., *J. Chem. Soc. Faraday Trans. 1* **78,** 3281 (1982).
5. Delmon, B., "Introduction à la Cinétique Hétérogène." Editions Technip, Paris, 1969.
6. Butler, M. A., and Ginley, D. S., *J. Electrochem. Soc.* **125,** 228 (1978).
7. Wang, E. Y., and Hsu, L., *J. Electrochem. Soc.* **125,** 1328 (1978).
8. Pan, C. A., and Ma, T. P., *J. Electronic Mater.* **10,** 43 (1981).
9. "Lange's Handbook of Chemistry" (Dean, J. A., Ed.), 12th. ed. McGraw–Hill, New York, 1979.